

Low-lying excited states in ^{62}Ge investigated by multinucleon knock-out reaction

Z Elekes^{1,2} , V Panin^{3,4}, T R Rodríguez⁵ , K Sieja^{6,7}, D S Ahn^{8,9}, A Al-Adili¹⁰, H Baba⁸, A I Stefanescu¹¹, K J Cook^{12,20}, Cs Dósa¹, N Fukuda⁸, J Gao^{8,13}, J Gibelin¹⁴ , K I Hahn^{9,15}, Z Halász¹, S W Huang^{8,13}, T Isobe⁸, M M Juhász^{1,2}, D Kim^{8,9,15}, T Kobayashi¹⁶, Y Kondo¹², Z Korkulu^{8,9}, A Kurihara¹², I Kuti¹, H Miki¹², K Miki¹⁶, T Motobayashi⁸ , H Otsu⁸, A Saastamoinen¹⁷, M Sasano⁸, H Sato⁸, N H Shadhin² , T Shimada¹², Y Shimizu⁸, I C Stefanescu^{11,18}, L Stuhl^{1,8,9}, H Suzuki⁸, H Takeda⁸, Y Togano^{8,19}, T Tomai¹², L Trache¹¹, D Tudor^{11,18}, T Uesaka⁸, Y Utsuki¹⁶, H Wang¹², A Yasuda¹², K Yoneda⁸ and Y Yoshitome¹²

¹ HUN-REN Institute for Nuclear Research (ATOMKI), PO Box 51, H-4001 Debrecen, Hungary

² Institute of Physics, Faculty of Science and Technology, University of Debrecen, Egyetem tér 1., H-4032 Debrecen, Hungary

³ Institut für Kernphysik, Technische Universität Darmstadt, 64289 Darmstadt, Germany

⁴ GSI Helmholtzzentrum für Schwerionenforschung GmbH, 64291 Darmstadt, Germany

⁵ Departamento de Estructura de la Materia, Física Térmica y Electrónica and IPARCOS, Complutense University of Madrid, 28040 Madrid, Spain

⁶ Université de Strasbourg, IPHC, 23 rue du Loess 67037 Strasbourg, France

⁷ CNRS, UMR7178, 67037 Strasbourg, France

⁸ RIKEN Nishina Center, 2-1 Hirosawa, Wako, Saitama 351-0198, Japan

⁹ Center for Exotic Nuclear Studies, Institute for Basic Science, Daejeon 34126, Republic of Korea

¹⁰ Uppsala University, PO Box 256, SE-751 05 Uppsala, Sweden

¹¹ Horia Hulubei National Institute for R&D in Physics and Nuclear Engineering (IFIN-HH), Magurele, 077025 Ilfov, Romania

¹² Department of Physics, Tokyo Institute of Technology, 2-12-1 O-Okayama, Meguro, Tokyo, 152-8551, Japan

¹³ State Key Laboratory of Nuclear Physics and Technology, School of Physics, Peking University, No. 5 Yiheyuan Road, Haidian district, 100871, Beijing, People's Republic of China

¹⁴ Université de Caen Normandie, ENSICAEN, CNRS/IN2P3, LPC Caen UMR6534, F-14000 Caen, France

¹⁵ Ewha Womans University, Seoul 120-750, Republic of Korea

¹⁶ Department of Physics, Tohoku University, Sendai 980-8578, Japan

¹⁷ Texas A&M University, Department of Physics and Astronomy, 578 University Drive College Station, TX 77843-4242, United States of America

¹⁸ Doctoral School of Physics, University of Bucharest, 405 Atomistilor Street, Măgurele, Ilfov, 077125, Romania

¹⁹ Department of Physics, Rikkyo University, 3-34-1 Nishi-Ikebukuro, Toshima, Tokyo 172-8501, Japan

E-mail: elekes@atomki.hu

Received 5 April 2024, revised 31 July 2024

Accepted for publication 15 August 2024

Published 4 September 2024



Abstract

The low-energy states of the proton-rich nucleus ^{62}Ge were studied by the multinucleon knock-out reaction $^{67}\text{Se}(^{12}\text{C},\text{X})^{62}\text{Ge}$ using a ^{12}C target. The analysis of the Doppler-corrected singles spectrum of the γ rays showed two transitions at 744(20) keV and 948(17) keV, which were found to be in coincidence with each other, forming a cascade and establishing two states at 948(17) keV and 1692(26) keV. The 744 keV transition was detected for the first time, and based on a comparison of the experimental data to shell-model and symmetry-conserving-configuration-mixing-model calculations, it connects the second and first 2^+ levels. The beyond-mean-field model suggests that these states belong to two different bands with triaxial features and similar deformation.

Keywords: 62-germanium, multinucleon knock-out, γ -ray spectroscopy, nuclear structure

1. Introduction

Since its first appearance in ^{16}O suggested by Morinaga [1], shape coexistence has been discovered throughout the nuclear chart. Recently, experimental results and theoretical approaches were reviewed [2, 3]. One of the most interesting regions where shape evolution and coexistence were identified are the neutron-deficient nuclei around the $N = Z$ line between the nickel and zirconium isotopic chains. From another point of view this region is also a fertile ground where the mirror energy difference can be experimentally studied, and the isospin non-conserving term of the nuclear interaction can be explored [4–8]. Furthermore, the astrophysical rp -process path goes through this region, and the structure of these nuclei is important to determine the key reactions for the understanding of type I x-ray bursts [9–12].

²⁰ Present address: Department of Nuclear Physics and Accelerator Applications, Research School of Physics, The Australian National University, Canberra, ACT 2600, Australia.

 Original content from this work may be used under the terms of the [Creative Commons Attribution 4.0 licence](#). Any further distribution of this work must maintain attribution to the author(s) and the title of the work, journal citation and DOI.

Along the $N = Z$ line, shape coexistence was experimentally found in ^{56}Ni [13], which was interpreted within Monte-Carlo-shell-model calculations [14]. For ^{60}Zn , a rotor is expected based on shell-model calculations [15], which is confirmed by the experimentally determined level energies of the yrast band [16] although no transition strengths were measured. ^{64}Ge was found to be unstable against triaxial deformation in the ground state [17, 18]. Two coexisting rotational bands with different moments of inertia were identified in ^{68}Se [19], and similarly shape coexistence was established in ^{72}Kr [20] and ^{76}Sr [21].

Beyond the $N = Z$ line, for $T_z = -1$ nuclei, the experimental information is scarce: only the yrast band is known up to spin/parity of 10^+ for ^{54}Ni [4]; one bound, likely the first 2^+ excited state, and some resonances were found in ^{58}Zn [10]; two transitions were observed in ^{74}Sr [8], nonetheless signs of shape coexistence were recently reported in ^{66}Se [22] and ^{70}Kr [7] based on the identification of their second 2^+ state and comparisons to theoretical calculations, which imply different deformations for the associated second bands.

For ^{62}Ge , until recently only a single experiment [6, 23] was available that mentioned two possible transitions at energies of 964 and 1321 keV. However, the existence of these transitions was uncertain because a thorough statistical analysis of the spectrum, which was largely contaminated by events from ^{62}Zn and ^{62}Ga , was not provided. A new paper uncovered several transitions by fusion-evaporation and inelastic scattering reactions for ^{62}Ge at energies of 965 keV, 1227 keV, 1505 keV, 2232 keV, and 1756 keV [24]. The 1756 keV transition was tentatively placed between the 2_2^+ and the ground state. However the transition between the 2_2^+ and the 2_1^+ levels, which was expected to be stronger based on the branching ratios of the mirror nucleus (59% for $2_2^+ \rightarrow 2_1^+$ and 41% for $2_2^+ \rightarrow 0_1^+$), was not seen. Therefore, our aim was to further study the low-energy level structure of ^{62}Ge by γ -ray spectroscopy from multinucleon knock-out reaction and clarify the location of the 2_2^+ level.

2. Experiment

The details of the experiment, which was performed at the Radioactive Isotope Beam Factory operated by the RIKEN Nishina Center and by the Center for Nuclear Study of the University of Tokyo, were discussed in our previous paper [22] however we repeat here some fundamental features for completeness. The radioactive species were produced by fragmentation from a beam of ^{78}Kr ions hitting a ^9Be target with a thickness of 2 mm at an intensity of 400 pnA and an energy of 345 MeV/u. The BigRIPS separator [25] was used to purify the radioactive ion beam and to identify the different nuclei using the standard procedure based on magnetic rigidity ($B\rho$), energy loss (ΔE) and time of flight (TOF) measurements discussed in more detail in an earlier publication [26]. After the beam tuning with reduced primary beam intensity of 40 pnA, the ionization chamber, used for determining energy loss, was removed because it could not handle the high total intensity of the radioactive cocktail beam (10^4 particle s $^{-1}$) during data collection. However, the separation of the ^{67}Se ions was monitored and provided with a 7.5σ in A/Q by the TOF and $B\rho$ information. The excited states of the nuclei in question were populated in a ^{12}C target with a thickness of 2 mm at one of the final focal planes of the separator which was surrounded by 100 CsI(Na) scintillator detectors of the CATANA array [27] to observe the prompt γ rays emitted during the deexcitation process. This array was energy-calibrated by radioactive sources, and a detection threshold of 100 keV was obtained in the laboratory system. An add-back procedure merging the hits closer than 10 cm and within a 10 ns time window was used to increase the photopeak efficiency to a value of around 15% in the 500–1500 keV energy range while the energy resolution was around 13% (FWHM value) for 1 MeV. The events were Doppler-corrected

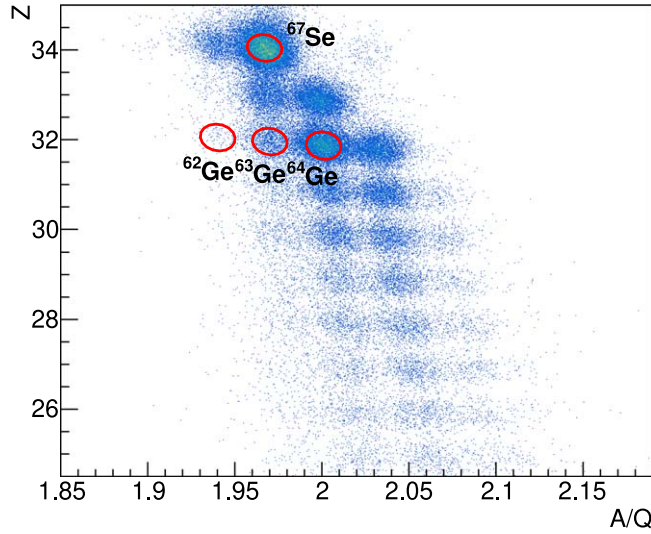


Figure 1. Identification of fragments with cuts on the incoming beam ^{67}Se and the Doppler-corrected γ rays with energies larger than 200 keV. Some of the fragment cuts applied when producing the γ -ray spectra are shown with red ellipses.

for the center-of-mass frame using the position information of the detectors relative to the carbon target and the beam velocity at the middle of the target. The beam-like ions were analyzed by the SAMURAI spectrometer [28] based on $B\rho$, ΔE , and TOF measurements. Multiwire drift chambers located upstream and downstream of the magnet served to determine the trajectories, and the magnetic rigidity was calculated using the multidimensional fit procedure of the ROOT framework [29]. A plastic scintillator array of 7 bars provided the energy loss and the time of flight. The identification of the fragments presented in figure 1 was based on the obtained 4.1σ separation in Z and 3.2σ separation in A/Q . The intensity and energy of the ^{67}Se ions entering the carbon target were 10^3 particle s^{-1} and about 250 MeV/u while the energy loss in the target was about 80 MeV/u.

3. Results

Figure 2 shows the Doppler-corrected singles spectrum for ^{64}Ge (panel A), ^{63}Ge (panel B), and ^{62}Ge (panel C) from the $^{67}\text{Se}(^{12}\text{C},\text{X})$ reaction. The smooth background, known to have two components (atomic process and scattered particles) from previous experiments [30, 31], was modeled by a double-exponential function with four free parameters, which proved to be successful with a similar scintillator array (see, e.g. [32–35]). The statistical confidence, energy, and intensity of the observed peaks were deduced by using our Geant4 [36] application, which provided the response function of the CATANA array for a γ ray emitted by the fast-moving projectile, taking into account the intrinsic experimental resolution of the CsI(Na) crystals. The resulting response functions were added together with individual scaling parameters plus the double-exponential background function to fit the spectrum using the likelihood method [37] of the ROOT framework [38], which gives more reliable results in comparison to the chi-square method for fitting spectra with low statistics [32, 39].

The spectrum for ^{64}Ge served as a benchmark with its known low-energy transitions. A total fit using four peaks of 571(6) keV, 677(6) keV, 901(5) keV, and 1146(6) keV with a

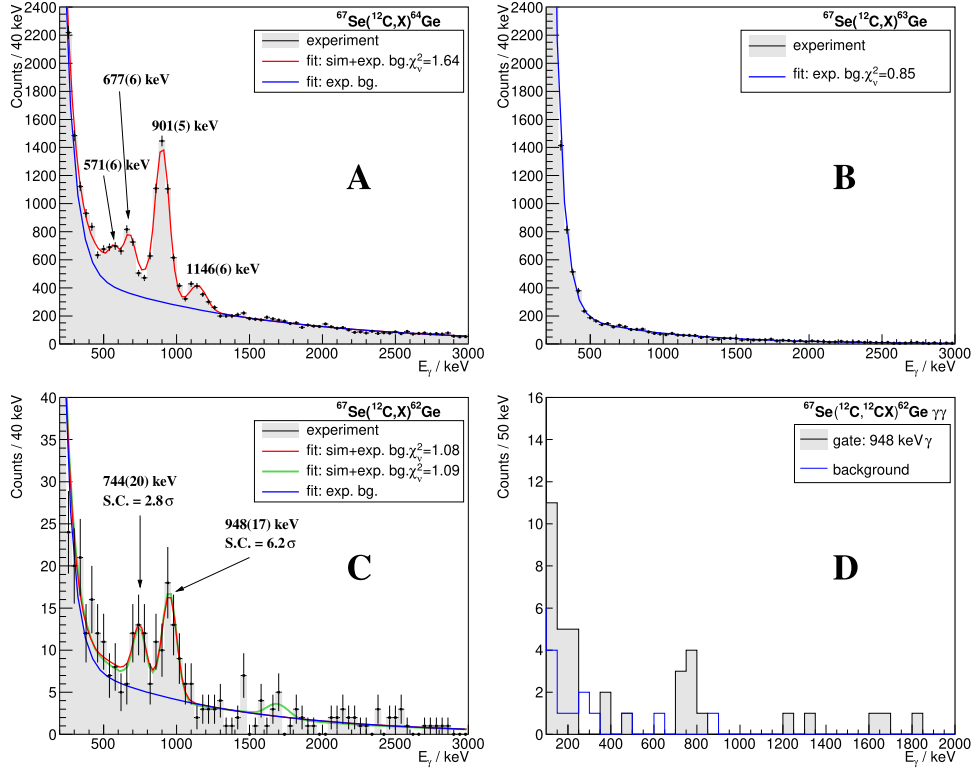


Figure 2. Doppler-corrected singles γ -ray spectrum for ^{64}Ge (A), ^{63}Ge (B), ^{62}Ge (C) and coincidence γ -ray spectrum for ^{62}Ge (D) using add-back procedure for the $^{67}\text{Se}(^{12}\text{C}, \text{X})$ multinucleon knock-out reaction. The data with error bars and shaded area represent the experimental spectrum, the red line is the simulation plus a double-exponential background, and the latter function (exponential background) is also plotted separately as a blue line. For panel C, an additional fit is provided (green line) assuming the spectrum contains also the 1692 keV transition between the 2_2^+ and 0_1^+ states (see text for details). The coincidence spectrum was created by selecting events in the $\gamma\gamma$ matrices in coincidence with the 948 keV γ ray, while the blue background spectrum was made by selecting a gate right beside the γ ray in question.

reduced χ^2 (χ^2_ν) of 1.64 was achieved presented by a red line (the background is shown by the blue line). The quoted uncertainties for the γ -ray energies include uncertainties arising from the statistics, the energy calibration (4 keV), the background estimation, and the Doppler correction. The uncertainty associated with the Doppler correction stems from the uncertainty of the velocity measurement (3 keV) and the angle of the detector elements of the array with respect to the beam direction. The latter was minimized by adjusting the position of the array in the analysis until transitions with well-known energies matched the literature value within 1 keV. The obtained energies are in a very good agreement with the ^{64}Ge γ -ray transition literature values of 576.2(3) keV, 677.0(3) keV, 901.5(3) keV, and 1150.8(4) keV corresponding to the decay of the four lowest-energy levels [40].

The spectrum of ^{63}Ge is also shown due to its proximity to ^{62}Ge and its high production from the $^{67}\text{Se} + ^{12}\text{C}$ reaction. This allows for the potential contamination of the ^{62}Ge spectrum to be identified. γ -ray peaks are not detected in the ^{63}Ge spectrum at energies above 500 keV,

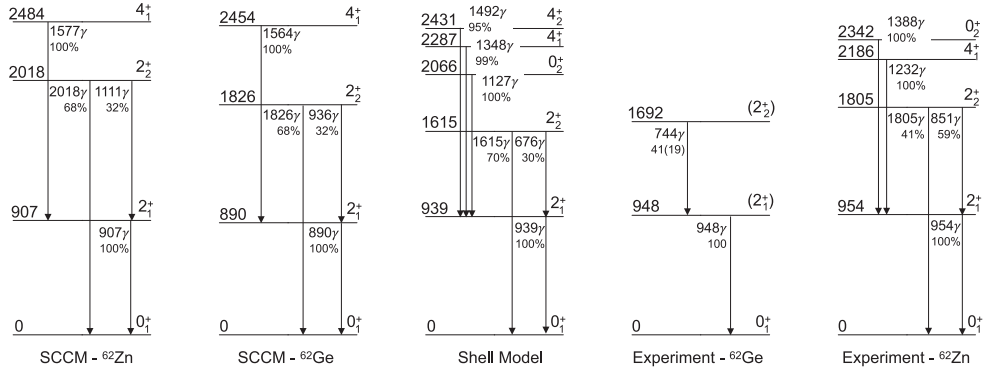


Figure 3. Partial level scheme of ^{62}Ge and ^{62}Zn up to around the proton separation energy of 2.29(15) MeV [46] from the symmetry-conserving-configuration-mixing model (SCCM), shell model (Coulomb term not included), the present data, and for the mirror nucleus. The γ -ray branching ratios are given for the theoretical and the mirror-nucleus level schemes while the efficiency-corrected intensity relative to the 948 keV transition is shown for the 744 keV transition in case of the experimental level scheme.

which is relevant for the spectrum of ^{62}Ge , or at energies below 500 keV. There is only one conference proceedings available in the literature where a single transition with an energy of 417.5(1) keV was reported [41] for ^{63}Ge . This was seen in the β -decay of ^{64}Se followed by the decay of one of the proton-unbound states of ^{64}As , so it is likely that the corresponding level in ^{63}Ge was not populated in our multinucleon knock-out reaction. It is also possible that the transition is undetectable due to the instrumental high background and the expected close location of many overlapping low-energy transitions based on the information on ^{65}Ge [42], which would result in an additional background without distinct peaks.

In the spectrum of ^{62}Ge , two peaks were identified at 744(20) keV and 948(17) keV with statistical confidences of 2.8σ and 6.2σ , respectively. The statistical confidence values changed by less than 0.2σ when the binning was changed. One of the transitions (948) is in agreement within the uncertainties with the 965 keV transition reported earlier [6, 23, 24]. The other 744 keV transition was not observed previously. From the constructed $\gamma\gamma$ matrix with a multiplicity of 2 for the CATANA array, a spectrum coincident with the 948 keV transition is shown in panel D of figure 2 (grey shaded). A peak appears at an energy of 759(27) keV consistent with 744 keV transition in the singles spectrum. A background spectrum in blue is also presented with a gate just displaced in energy from the 948 keV transition. This confirms that the two observed transitions form a cascade.

4. Discussion and interpretation of the results

To interpret the observed data, a shell-model calculation was performed to obtain the energy spectra and the electromagnetic transition rates by the ANTOINE code [43, 44]. The applied interaction was JUN45 (Coulomb term not included) which was developed for the description of nuclei in the $p_{1/2}f_{5/2}g_{9/2}$ valence space with the proposed effective charges of $e_p = 1.5e$ and $e_n = 1.1e$ when evaluating the E2 transitions [45]. The calculated level scheme and the γ -ray branching ratios of the main transitions up to the proton separation energy of 2.29(15) MeV [46] are plotted in figure 3, marked as ‘Shell Model’, together with the information known for the mirror nucleus ^{62}Zn .

To gain further insight into intrinsic shapes of ^{62}Ge , calculations were carried out using the symmetry-conserving configuration mixing (SCCM) method with the Gogny D1S energy density functional (EDF) [47, 48]. The objective of this method is to obtain variational approximations for the exact wave functions. In the present case, the intrinsic HFB states were obtained by minimizing the particle-number projected energy for different values of the quadrupole deformation parameters, β_2 . As these are no-core calculations, no effective quadrupole operators were needed to define the triaxial map (β_2, γ) or to calculate the electromagnetic properties.

Based on the larger intensity of the 948 keV transition and the comparison to the level schemes of the theoretical models and the mirror-nucleus, this transition connects the 2_1^+ state and the ground state in agreement with the earlier findings [6, 23, 24]. The 744 keV transition, which coincides with the 948 keV transition, establishes a state at an energy of 1692(26) keV. This state is a good candidate for the second 2^+ state because a very similar energy has been observed in the mirror nucleus, and the theoretical calculations also align with this assignment. Furthermore, a transition at 1756(13) keV was obtained in the earlier proton knock-out reaction which was tentatively proposed to connect the 2_2^+ state and the ground state [24]. However, the expected stronger $2_2^+ \rightarrow 2_1^+$ transition was not observed due to the large Compton background. On the other hand, here the $2_2^+ \rightarrow 0_1^+$ transition was not seen, which is due to the low statistics as it is demonstrated in panel C of figure 2 by the green fit which is performed in a way that the scaling parameter of the response function of the CATANA array for the $2_2^+ \rightarrow 0_1^+$ transition (1692 keV) was bound to that of the $2_2^+ \rightarrow 2_1^+$ transition (744 keV) using a multiplicative factor of $41/59 = 0.69$ originating from the branching ratios for the 2_2^+ level of the mirror nucleus. The change in the goodness of the fit (from 1.08 to 1.09) is negligible adding this $2_2^+ \rightarrow 0_1^+$ transition, which means that the statistics in the present spectrum does not allow to confirm or exclude its existence.

The experimental mirror energy difference of the 2_2^+ , defined as $E(2_2^+ T_z = -1) - E(2_2^+ T_z = +1)$, for the ^{62}Ge - ^{62}Zn pair is $-113(26)$ keV which is consistent with the negative values measured for such pairs in the region: $-166(6)$ keV (^{58}Zn - ^{58}Ni) [10, 49], $-22(6)$ keV (^{66}Se - ^{66}Ge) [22, 50], and $-122(11)$ keV (^{70}Kr - ^{70}Se) [7, 51].

According to the SCCM calculations, the collective quadrupole properties are mostly dictated by the total particle-number-projected energy surface (PNVAP-TES) represented in figure 4(f), where a clear triaxial minimum at $(\beta_2, \gamma) = (0.25, 20^\circ)$ was observed. Then, the final energies, branching ratios, and collective wave functions were obtained after performing angular momentum projection and shape mixing. Hence, the SCCM calculations predicted a $\Delta J = 2$ ground-state-band ($0_1^+, 2_1^+, 4_1^+, \dots$) and a $\Delta J = 1$ γ -band ($2_2^+, 3_1^+, 4_2^+, \dots$) built on top of the triaxial configurations where the minimum of the PNVAP-TES was obtained (see the collective wave functions shown in figure 4(a)-(d)). It is worth noting that a significantly different band was also identified, where the band head is the 0_2^+ state which is a mix of modestly deformed configurations ($\beta_2 = 0.18$) and a contribution from a deformed state at $(\beta_2, \gamma) = (0.5, 20^\circ)$ (see figure 4(e)). Additionally, it is also interesting that this 0_2^+ state is located at about 5 MeV in SCCM and at a very low energy (about 2 MeV) in the shell model. This presents a good opportunity for a future experiment to look for shape coexistence in ^{62}Ge .

Finally, the SCCM calculations also predicted a similar collective structure (triaxial ground-state-band and γ -band) for the mirror isotope ^{62}Zn (not shown). Due to the Coulomb interaction, that was inherent in this method, slightly larger excitation energies were obtained for the 2_1^+ and 2_2^+ states with respect to that of ^{62}Ge , in agreement with the experimental trend

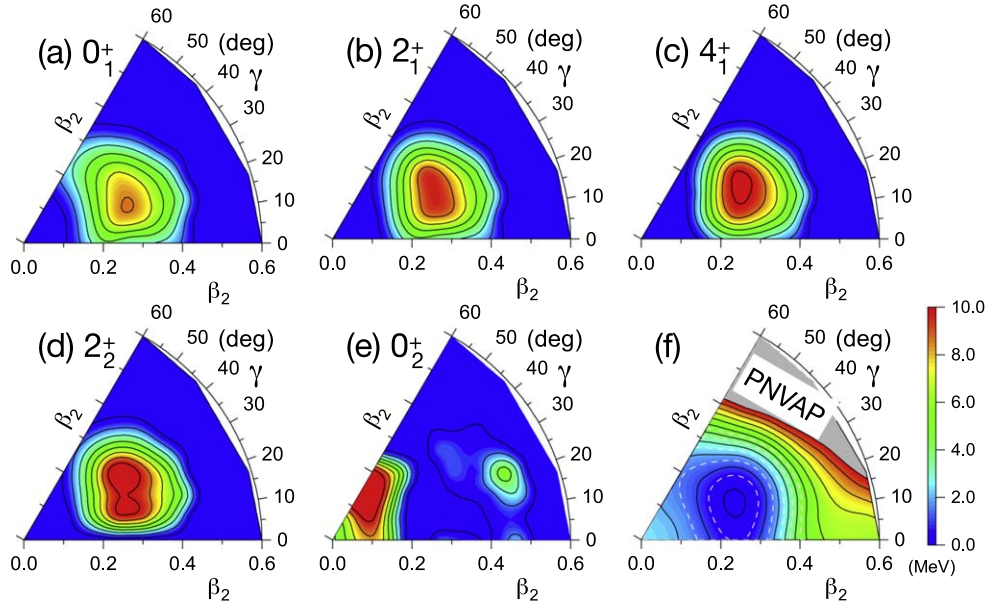


Figure 4. (a)–(e) SCCM collective wave functions, and, (f) particle-number variation-after-projection total energy surface, as a function of the quadrupole (β_2 , γ) deformations, computed with Gogny D1S EDF. See text for more details.

(see figure 3). The branching ratios for the decay of the 2_2^+ state were calculated to be the same in ^{62}Zn and ^{62}Ge but they are somewhat different from the experimental values of ^{62}Zn .

5. Summary

The low-energy nuclear structure of ^{62}Ge was studied by the multinucleon knock-out reaction using a thin ^{12}C target. Two transitions were observed in coincidence with each other, establishing two excited states. These states were assigned to the first and second 2^+ levels based on a comparison to shell-model and beyond-mean-field-model calculations, as well as information on low-lying states in the mirror nucleus ^{62}Zn . According to our SCCM calculations, the observed states belong to the triaxial ground state band and its associated γ -band with similar deformations. Another significantly different band built on the 0_2^+ state, which is predicted to be located at very different energies by the two theoretical approaches, calls for further work to explore this exotic feature.

Acknowledgments

ZE, CsD, ZH, GyH, IK, LS and MMJ were supported by NKFIH under projects TKP2021-NKTA-42, K147010, and 2021-4.1.2-NEMZ_KI-2021-00005. TRR acknowledges funding from the Spanish MICIN under contract PID2021-127890NB-I00 and support from GSI-Darmstadt computing facilities. YT was supported by JSPS Grant-in-Aid for Scientific Research Grants No. JP21H01114. KJC acknowledges the JSPS International Fellowship for Research in Japan, hosted by the Tokyo Institute of Technology. DSA, KIH and DK acknowledge the support from the IBS grant funded by the Korea government (No. IBS-R031-D1). VP

acknowledges the Kakenhi Grant-in-Aid for Young Scientists B No. 16K17719. AA acknowledges the JSPS International Fellowships for their travel support. ICS, LT, DT and AIS were supported by projects PNIII-P4-ID-PCE-2016-0743 and PNIII/P5/P5.2 nr. 02/FAIR-RO.

Data availability statement

The data cannot be made publicly available upon publication because no suitable repository exists for hosting data in this field of study. The data that support the findings of this study are available upon reasonable request from the authors.

ORCID iDs

Z Elekes  <https://orcid.org/0000-0003-0571-8719>
 T R Rodríguez  <https://orcid.org/0000-0002-3516-8239>
 J Gibelin  <https://orcid.org/0000-0001-6751-3714>
 T Motobayashi  <https://orcid.org/0000-0002-7661-3941>
 N H Shadhin  <https://orcid.org/0009-0001-3954-2734>

References

- [1] Morinaga H 1956 *Phys. Rev.* **101** 254–8
- [2] Garrett P E, Zielińska M and Clément E 2022 *Prog. Part. Nucl. Phys.* **124** 103931
- [3] Bonatsos D, Martinou A, Peroulis S K, Mertzimekis T J and Minkov N 2023 *Atoms* **11** 117
- [4] Rudolph D *et al* 2022 *Phys. Lett. B* **830** 137144
- [5] Fernández A *et al* 2021 *Phys. Lett. B* **823** 136784
- [6] Rudolph D, Johansson E, Andersson L L, Ekman J, Fahlander C and du Rietz R 2005 *Nucl. Phys. A* **752** 241–50
- [7] Wimmer K *et al* 2018 *Phys. Lett. B* **785** 441–6
- [8] Henderson J *et al* 2014 *Phys. Rev. C* **90** 051303
- [9] Fisker J, Barnard V, Görres J, Langanke K, Martínez-Pinedo G and Wiescher M 2001 *At. Data Nucl. Data Tables* **79** 241–92
- [10] Langer C *et al* 2014 *Phys. Rev. Lett.* **113** 032502
- [11] Parikh A, José J, Sala G and Iliadis C 2013 *Prog. Part. Nucl. Phys.* **69** 225–53
- [12] Rehm K E *et al* 1998 *Phys. Rev. Lett.* **80** 676–9
- [13] Rudolph D *et al* 1999 *Phys. Rev. Lett.* **82** 3763–6
- [14] Mizusaki T, Otsuka T, Utsuno Y, Honma M and Sebe T 1999 *Phys. Rev. C* **59** R1846–50
- [15] Zuker A P, Poves A, Nowacki F and Lenzi S M 2015 *Phys. Rev. C* **92** 024320
- [16] de Angelis G *et al* 1998 *Nucl. Phys. A* **630** 426–33
- [17] Ennis P, Lister C, Gelletly W, Price H, Varley B, Butler P, Hoare T, Ćwiołk S and Nazarewicz W 1991 *Nucl. Phys. A* **535** 392–424
- [18] Starosta K *et al* 2007 *Phys. Rev. Lett.* **99** 042503
- [19] Fischer S M, Balamuth D P, Hausladen P A, Lister C J, Carpenter M P, Seweryniak D and Schwartz J 2000 *Phys. Rev. Lett.* **84** 4064–7
- [20] Iwasaki H *et al* 2014 *Phys. Rev. Lett.* **112** 142502
- [21] Lemasson A *et al* 2012 *Phys. Rev. C* **85** 041303
- [22] Elekes Z *et al* 2023 *Phys. Lett. B* **844** 138072
- [23] Johansson E 2004 *The Quest for Excited States in ⁶²Ge* Lund University Master's thesis <https://nuclear.lu.se/fileadmin/nuclear/Grundlaeggande/Theeses/Johansson.pdf>
- [24] Wimmer K *et al* 2023 *Phys. Lett. B* **847** 138249
- [25] Kubo T *et al* 2012 *Prog. Theor. Exp. Phys.* **2012** 03C003
- [26] Fukuda N, Kubo T, Ohnishi T, Inabe N, Takeda H, Kameda D and Suzuki H 2013 *Nucl. Instrum. Methods Phys. Res. B* **317** 323–32
- [27] Togano Y *et al* 2020 *Nucl. Instrum. Methods Phys. Res. B* **463** 195–7

[28] Kobayashi T *et al* 2013 *Nucl. Instrum. Methods Phys. Res. B* **317** 294–304 XVIth Int. Conf. on ElectroMagnetic Isotope Separators and Techniques Related to their Applications, December 2–7, 2012 at Matsue, Japan

[29] Root multidimfit <https://root.cern.ch/doc/master/classTMultiDimFit.html>

[30] Doornenbal P 2012 *Prog. Theor. Exp. Phys.* **2012** 03C004

[31] Cortés M L *et al* 2018 *Phys. Rev. C* **97** 044315

[32] Liu H N *et al* 2019 *Phys. Rev. Lett.* **122** 072502

[33] Sun Y *et al* 2020 *Phys. Lett. B* **802** 135215

[34] Cortés M *et al* 2020 *Phys. Lett. B* **800** 135071

[35] Cortés M L *et al* 2020 *Phys. Rev. C* **102** 064320

[36] Agostinelli S *et al* 2003 *Nucl. Instrum. Methods Phys. Res. A* **506** 250–303

[37] Baker S and Cousins R D 1984 *Nucl. Instrum. Methods Phys. Res.* **221** 437–42

[38] Antcheva I *et al* 2009 *Comput. Phys. Commun.* **180** 2499–512

[39] Olivier L 2017 *Nuclear Structure in the Vicinity of ⁷⁸Ni: In-beam Gamma-ray Spectroscopy of ⁷⁹Cu through Proton Knockout* Université Paris-Saclay PhD Thesis, <https://tel.archives-ouvertes.fr/tel-01637435/document>

[40] Singh B and Chen J 2021 *Nucl. Data Sheets* **178** 41–537

[41] Rubio B *et al* 2019 *J. Phys. Conf. Ser.* **1308** 012018

[42] Browne E and Tuli J 2010 *Nucl. Data Sheets* **111** 2425–553

[43] Caurier E and Nowacki F 1999 *Acta Phys. Pol. B* **30** 705–14

[44] Caurier E, Martínez-Pinedo G, Nowacki F, Poves A and Zuker A P 2005 *Rev. Mod. Phys.* **77** 427–88

[45] Honma M, Otsuka T, Mizusaki T and Hjorth-Jensen M 2009 *Phys. Rev. C* **80** 064323

[46] Wang M, Huang W, Kondev F, Audi G and Naimi S 2021 *Chin. Phys. C* **45** 030003

[47] Rodríguez T R and Egido J L 2010 *Phys. Rev. C* **81** 064323

[48] Robledo L M, Rodríguez T R and Rodríguez-Guzmán R R 2018 *J. Phys. G: Nucl. Part. Phys.* **46** 013001

[49] Nesaraja C D, Geraedts S D and Singh B 2010 *Nucl. Data Sheets* **111** 897–1092

[50] Browne E and Tuli J 2010 *Nucl. Data Sheets* **111** 1093–209

[51] Gündal G and McCutchan E 2016 *Nucl. Data Sheets* **136** 1–162